Available online at www.sciencedirect.com
ScienceDirect
Journal of Sound and Vibration 305 (2007) 563–581
JOURNAL OF SOUND AND VIBRATION
www.elsevier.com/locate/jsvi

Parametric vibration of thin-walled composite beams with shear deformation

Sebastián P. Machado[a,b,*], Carlos P. Filipich[a], Víctor H. Cortínez[a,b]

[a]Grupo Análisis de Sistemas Mecánicos, Facultad Regional Bahía Blanca, Universidad Tecnológica Nacional, 11de abril 461, B8000LMI Bahía Blanca, Argentina
[b]CONICET, Argentina

Received 24 May 2006; received in revised form 29 December 2006; accepted 7 March 2007
Available online 2 July 2007

Abstract

The dynamic stability of thin-walled composite beams, considering shear deformation, subjected to axial external force, has been investigated in this paper. The analysis is based on a small strain and moderate rotation theory, which is formulated through the adoption of a second-order displacement field. The Galerkin's method is used in order to discretize the governing equation and the Bolotin's method is applied to determine the regions of dynamic instability of a simply supported beam. The regions of instability are evaluated, and are expressed in non-dimensional terms. The influence of the longitudinal vibration on the unstable regions has been investigated. The numerical results show that this effect has large influence when the forcing frequency approaches to the natural longitudinal frequency, obtaining parametric instability regions substantially wider. Besides, the effect of shear flexibility is also analyzed for different laminate stacking sequence, considering open and closed cross-section beams.

1. Introduction

Thin-walled beam structures made of advanced anisotropic composite materials are increasingly found in the design of the aircraft wing, helicopter blade, axles of vehicles and so on, due to their outstanding engineering properties, such as high strength/stiffness to weight ratios and favorable fatigue characteristics. The interesting possibilities provided by fiber reinforced composite materials can be used to enhance the response characteristics of such structures that operate in complex environmental conditions. Besides, the composite thin-walled beam members are widely used in aerospace, automobile and civil architecture industries. The new generation of these constructions should be designed to work in a safe way under complex environmental conditions, and to experience higher performance than the conventional systems. The theory of dynamic stability represents a specific aspect of the stability of the motion, which is related the theory of vibrations and stability of mechanical systems.

*Corresponding author. Grupo Análisis de Sistemas Mecánicos, Facultad Regional Bahía Blanca, Universidad Tecnológica Nacional, 11de abril 461, B8000LMI Bahía Blanca, Argentina. Tel.: +54 0291 4555220; fax: +54 0291 4555311.
E-mail addresses: smachado@frbb.utn.edu.ar (S.P. Machado), vcortine@frbb.utn.edu.ar (V.H. Cortínez).

0022-460X/$ - see front matter
doi:10.1016/j.jsv.2007.03.092

The dynamic instability of elastic structural elements, such as rods, beams and columns, induced by parametric excitation has been investigated by many researchers. Extensive bibliographies on this subject were given by Evan-Iwanowski [1] and Nayfeh and Mook [2]. Bolotin [3] provided a general introduction to analyze the dynamic stability problems of various structural elements.

The Mathieu–Hill equation [1,3] is obtained while resolving the parametric vibration of a beam subjected to a compressive dynamic force. Nayfeh and Mook [2], used the perturbation method to solve Mathieu–Hill's equation, in order to analyze the behavior of an elastic system under parametric excitation. They established a criterion to yield the transition curves by determining the characteristic exponents in the solution.

In relation to thin-walled beams, Gol'denblat [4] investigated the problem of the stability of a compressed thin-walled rod symmetrical about one axis. The problem was reduced to a system of two differential equations. Tso [5] studied the problem of longitudinal–torsional stability, while Mettler [6] and Ghobarah and Tso [7] studied the problem of bending–torsional stability of thin-walled beams. Bolotin [3,8] and Popelar [9,10] discussed the dynamic stability of thin-walled beams; typical I and H sections were considered. Hasan and Barr [11] evaluated regions of instability of thin-walled beams of equal angle-section, considering axial and transverse excitation in a cantilever beam. Although a number of authors have investigated the problem of dynamic stability of thin-walled beams, the effects of shear deformation has been assumed to be small and neglected in the analysis.

In spite of the practical interest and future potential of the thin-walled composite beam structures, particularly in the context of aerospace and mechanical applications, the main body of the available investigations has devoted to study the dynamic response behavior of composite beams of solid sections [12,13]. Therefore, it seems that, to the best knowledge of the authors, there is no work investigating the problem of dynamic stability of composite thin-walled beams subjected to axial excitation.

On the other hand, the contribution to the axial displacement from second-order effects gives rise to a longitudinal inertia force, which must be taken into account during the derivation of the equations of motion. Longitudinal vibrations can influence the regions of dynamic stability [3,14]. In the present paper, the contribution of this effect on the dynamic behavior is included.

The analysis is based on a second-order geometrically nonlinear shear deformable beam theory, which is a simplified version of the theory recently developed by the authors [15,16], that is valid for symmetric balanced and especially orthotropic laminates [17,18]. The model is based on a small strain and moderate rotation theory, which is formulated through the adoption of a second-order displacement field. The adoption of a first-order approximation in the displacement field may lead to incorrect expressions for the equations of motion and to inaccurate predictions of the dynamic behavior of thin-walled beams [19].

The Galerkin's method is used in order to discretize the governing equation and the Bolotin's method is applied to determine the regions of dynamic instability of a simply supported beam. The regions of instability are evaluated, and are expressed in non-dimensional terms.

The purpose of the present investigation is the determination of the regions of dynamic instability of simply supported thin-walled composite beam subjected to an axial excitation and considering open and closed cross-section. The influence of shear deformation, natural longitudinal vibration and load static parameter on the unstable regions is analyzed, considering different laminate stacking sequences.

2. Kinematics

A straight thin-walled composite beam with an arbitrary cross-section is considered (Fig. 1). The points of the structural member are referred to a Cartesian coordinate system $(x, \bar{y}, \bar{z})$, where the x-axis is parallel to the longitudinal axis of the beam while $\bar{y}$ and $\bar{z}$ are the principal axes of the cross-section. The axes y and z are parallel to the principal ones but having their origin at the shear center (SR) (defined according to Vlasov's theory of isotropic beams). The coordinates corresponding to points lying on the middle line are denoted as Y and Z (or $\bar{Y}$ and $\bar{Z}$). In addition, a circumferential coordinate s and a normal coordinate n are introduced on the middle contour of the cross-section:

$$\bar{y}(s,n) = \bar{Y}(s) - n\frac{\mathrm{d}Z}{\mathrm{d}s}, \quad \bar{z}(s,n) = \bar{Z}(s) + n\frac{\mathrm{d}Y}{\mathrm{d}s}, \tag{1}$$

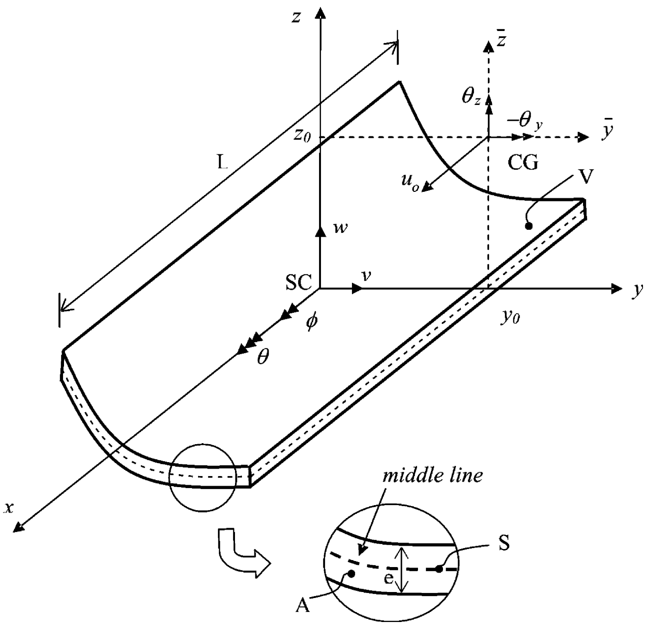

Fig. 1. Coordinate system of the cross-section and notation for displacement measures.

$$y(s,n) = Y(s) - n\frac{dZ}{ds}, \quad z(s,n) = Z(s) + n\frac{dY}{ds}. \tag{2}$$

On the other hand, y_0 and z_0 are the centroidal coordinates measured with respect to the SR:

$$\bar{y}(s,n) = y(s,n) - y_0, \quad \bar{z}(s,n) = z(s,n) - z_0. \tag{3}$$

The present structural model is based on the following assumptions [20]:

(1) The cross-section contour is rigid in its own plane.
(2) The warping distribution is assumed to be given by the Saint-Venant function for isotropic beams.
(3) Flexural rotations (about the $\bar{y}$ and $\bar{z}$ axes) and twist ϕ of the cross-section are assumed to be moderate.
(4) Shell force and moment resultants corresponding to the circumferential stress σ_{ss} and the force resultant corresponding to γ_{ns} are neglected.
(5) The curvature at any point of the shell is neglected.
(6) Twisting linear curvature of the shell is expressed according to the classical plate theory.
(7) The laminate stacking sequence is assumed to be symmetric and balanced, or especially orthotropic [17].

One the first paper on geometrically nonlinear theory was presented by Bhaskar and Librescu [21] for thin-walled composite beams. The nonlinear model is based on the hypothesis that the flexural displacement are finite and the twist of the cross-section can be arbitrary large.

According to the hypotheses of the present structural model, the displacement field proposed Eq. (4) is based on the principle of semitangential rotation defined by Argyris [22] to avoid the difficulty due to the noncommutative nature of rotations:

$$\begin{aligned} u_x &= u_o - \theta_z\bar{y} - \theta_y\bar{z} + \phi\theta_z z - \phi\theta_y y + \omega\left[\theta - \tfrac{1}{2}\left(\theta_y'\theta_z - \theta_y\theta_z'\right)\right], \\ u_y &= v - \phi z + \tfrac{1}{2}\left(-\phi^2 y - \theta_z^2\bar{y} - \theta_z\theta_y\bar{z}\right), \\ u_z &= w + \phi y + \tfrac{1}{2}\left(-\phi^2 z - \theta_y^2\bar{z} - \theta_z\theta_y\bar{y}\right). \end{aligned} \tag{4}$$

This expression is a second-order approximation of the displacement field proposed by the authors in Refs. [15,16]. On the other hand, neglecting the shear flexibility ($\theta_z = v'$, $\theta_y = w'$ and $\theta = \phi'$), the present displacement field coincides with that developed by Fraternali and Feo [23], who formulated a moderate rotation theory of thin-walled composite beams generalizing the infinitesimal theory of sectorial areas by Vlasov. Besides, a similar displacement field obtained by means of a second-order rotation matrix was used by Pi and Bradford [19] to show the effects of approximations in analysis of open thin-walled beams.

In the above expressions, ϕ, θ_y and θ_z are measures of the rotations about the SC axis, $\bar{y}$ and $\bar{z}$ axes, respectively; θ represents the warping variable of the cross-section. Furthermore, the superscript 'prime' denotes derivation with respect to the variable x. The warping function ω of the thin-walled cross-section may be defined as

$$\omega(s,n) = \omega_p(s) + \omega_s(s,n), \tag{5}$$

where ω_p and ω_s are the contour warping function and the thickness warping function, respectively. They are defined in the form [24,25]

$$\omega_p(s) = \frac{1}{S}\left[\int_0^S \left(\int_{s_0}^s [r(\sigma) - \psi(\sigma)]\,\mathrm{d}\sigma\right)\mathrm{d}s\right] - \int_{s_0}^s [r(\sigma) - \psi(\sigma)]\,\mathrm{d}\sigma, \quad \omega_s(s,n) = -nl(s), \tag{6a,b}$$

where σ is a dummy variable, and

$$r(s) = -Z(s)\frac{\mathrm{d}Y}{\mathrm{d}s} + Y(s)\frac{\mathrm{d}Z}{\mathrm{d}s}, \tag{7}$$

$$l(s) = Y(s)\frac{\mathrm{d}Y}{\mathrm{d}s} + Z(s)\frac{\mathrm{d}Z}{\mathrm{d}s}, \tag{8}$$

where $r(s)$ represents the perpendicular distance from the SC to the tangent at any point of the mid-surface contour, and $l(s)$ represents the perpendicular distance from the SC to the normal at any point of the mid-surface contour, as shown in Fig. 1.

In Eq. (6), Ψ is the shear strain at the middle line, obtained by means of the Saint-Venant theory of pure torsion for isotropic beams, and normalized with respect to $\mathrm{d}\phi/\mathrm{d}x$ [25]. For the case of open sections $\Psi = 0$.

3. The strain field

The displacements with respect to the curvilinear system (x, s, n) are obtained by means of the following expressions:

$$\bar{U} = u_x(x,s,n), \tag{9}$$

$$\bar{V} = u_y(x,s,n)\frac{\mathrm{d}Y}{\mathrm{d}s} + u_z(x,s,n)\frac{\mathrm{d}Z}{\mathrm{d}s}, \tag{10}$$

$$\bar{W} = -u_y(x,s,n)\frac{\mathrm{d}Z}{\mathrm{d}s} + u_z(x,s,n)\frac{\mathrm{d}Y}{\mathrm{d}s}. \tag{11}$$

The three non-zero components ε_{xx}, ε_{xs}, ε_{xn} of the Green's strain tensor are given by

$$\varepsilon_{xx} = \frac{\partial\overline{U}}{\partial x} + \frac{1}{2}\left[\left(\frac{\partial\overline{U}}{\partial x}\right)^2 + \left(\frac{\partial\overline{V}}{\partial x}\right)^2 + \left(\frac{\partial\overline{W}}{\partial x}\right)^2\right], \tag{12}$$

$$\varepsilon_{xs} = \frac{1}{2}\left[\frac{\partial\overline{U}}{\partial s} + \frac{\partial\overline{V}}{\partial x} + \frac{\partial\overline{U}}{\partial x}\frac{\partial\overline{U}}{\partial s} + \frac{\partial\overline{V}}{\partial x}\frac{\partial\overline{V}}{\partial s} + \frac{\partial\overline{W}}{\partial x}\frac{\partial\overline{W}}{\partial s}\right], \tag{13}$$

$$\varepsilon_{xn} = \frac{1}{2}\left[\frac{\partial\overline{U}}{\partial n} + \frac{\partial\overline{W}}{\partial x} + \frac{\partial\overline{U}}{\partial x}\frac{\partial\overline{U}}{\partial n} + \frac{\partial\overline{V}}{\partial x}\frac{\partial\overline{V}}{\partial n} + \frac{\partial\overline{W}}{\partial x}\frac{\partial\overline{W}}{\partial n}\right]. \tag{14}$$

Substituting Eq. (4) into Eqs. (9)–(11) and then into Eqs. (12)–(14), employing the relations expressed in Eqs. (1)–(3) and Eqs. (5)–(8), after simplifying some higher-order terms, the components of the strain tensor are expressed in the following form:

$$\varepsilon_{xx} = \varepsilon_{xx}^{(0)} + n\kappa_{xx}^{(1)}, \quad \gamma_{xs} = 2\varepsilon_{xs} = \gamma_{xs}^{(0)} + n\kappa_{xs}^{(1)}, \quad \gamma_{xn} = 2\varepsilon_{xn} = \gamma_{xn}^{(0)}, \tag{15}$$

where

$$\begin{aligned}\varepsilon_{xx}^{(0)} &= u_o' + \tfrac{1}{2}\left(v'^2 + w'^2\right) - y_0\theta_y'\phi + z_0\theta_z'\phi + \overline{Y}\left(-\theta_z' - \theta_y'\phi\right) + \overline{Z}\left(-\theta_y' + \theta_z'\phi\right) \\ &\quad + \omega_p\left[\theta' - \tfrac{1}{2}\left(\theta_z\theta_y'' - \theta_y\theta_z''\right)\right] + \tfrac{1}{2}\phi'^2\left(Y^2 + Z^2\right),\end{aligned} \tag{16}$$

$$\kappa_{xx}^{(1)} = -\frac{\mathrm{d}Z}{\mathrm{d}s}\left(-\theta_z' - \theta_y'\phi\right) + \frac{\mathrm{d}Y}{\mathrm{d}s}\left(-\theta_y' + \theta_z'\phi\right) - l\left[\theta' - \frac{1}{2}\left(\theta_z\theta_y'' - \theta_y\theta_z''\right)\right] - r\phi'^2, \tag{17}$$

$$\begin{aligned}\gamma_{xs}^{(0)} &= \frac{\mathrm{d}Y}{\mathrm{d}s}\left[v' - \theta_z - z_0\frac{1}{2}\left(\theta_z\theta_y' - \theta_y\theta_z'\right)\right] + \frac{\mathrm{d}Z}{\mathrm{d}s}\left[w' - \theta_y + y_0\frac{1}{2}\left(\theta_z\theta_y' - \theta_y\theta_z'\right)\right] \\ &\quad + (r - \psi)(\phi' - \theta) + \psi\left[\phi' - \frac{1}{2}\left(\theta_z\theta_y' - \theta_y\theta_z'\right)\right],\end{aligned} \tag{18}$$

$$\kappa_{xs}^{(1)} = -2\left[\phi' - \tfrac{1}{2}\left(\theta_z\theta_y' - \theta_y\theta_z'\right)\right], \tag{19}$$

$$\gamma_{xn}^{(0)} = -\frac{\mathrm{d}Z}{\mathrm{d}s}\left[v' - \theta_z - z_0\frac{1}{2}\left(\theta_z\theta_y' - \theta_y\theta_z'\right)\right] + \frac{\mathrm{d}Y}{\mathrm{d}s}\left[w' - \theta_y + y_0\frac{1}{2}\left(\theta_z\theta_y' - \theta_y\theta_z'\right)\right] + l(\phi' - \theta). \tag{20}$$

4. Variational formulation

Taking into account the adopted assumptions, the principle of virtual work for a composite shell may be expressed in the form [20,26]

$$\begin{aligned}&\iint\left(N_{xx}\delta\varepsilon_{xx}^{(0)} + M_{xx}\delta\kappa_{xx}^{(1)} + N_{xs}\delta\gamma_{xs}^{(0)} + M_{xs}\delta\kappa_{xs}^{(1)} + N_{xn}\delta\gamma_{xn}^{(0)}\right)\mathrm{d}s\,\mathrm{d}x \\ &\quad - \iiint\rho\left(\ddot{u}_x\delta u_x + \ddot{u}_y\delta u_y + \ddot{u}_z\delta u_z\right)\mathrm{d}s\,\mathrm{d}n\,\mathrm{d}x \\ &\quad - \iint(\bar{q}_x\delta\bar{u}_x + \bar{q}_y\delta\bar{u}_y + \bar{q}_z\delta\bar{u}_z)\,\mathrm{d}s\,\mathrm{d}x - \iint(\bar{p}_x\delta u_x + \bar{p}_y\delta u_y + \bar{p}_z\delta u_z)\Big|_{x=0}\mathrm{d}s\,\mathrm{d}n \\ &\quad - \iint(\bar{p}_x\delta u_x + \bar{p}_y\delta u_y + \bar{p}_z\delta u_z)\Big|_{x=L}\mathrm{d}s\,\mathrm{d}n - \iiint(\bar{f}_x\delta u_x + \bar{f}_y\delta u_y + \bar{f}_z\delta u_z)\,\mathrm{d}s\,\mathrm{d}n\,\mathrm{d}x = 0,\end{aligned} \tag{21}$$

where N_{xx}, N_{xs}, M_{xx}, M_{xs} and N_{xn} are the shell stress resultants defined according to the following expressions:

$$\begin{aligned}&N_{xx} = \int_{-e/2}^{e/2}\sigma_{xx}\,\mathrm{d}n, \quad M_{xx} = \int_{-e/2}^{e/2}(\sigma_{xx}n)\,\mathrm{d}n, \\ &N_{xs} = \int_{-e/2}^{e/2}\sigma_{xs}\,\mathrm{d}n, \quad M_{xs} = \int_{-e/2}^{e/2}(\sigma_{xs}n)\,\mathrm{d}n, \quad N_{xn} = \int_{-e/2}^{e/2}\sigma_{xn}\,\mathrm{d}n.\end{aligned} \tag{22}$$

The beam is subjected to wall surface tractions $\bar{q}_x$, $\bar{q}_y$ and $\bar{q}_z$ specified per unit area of the undeformed middle surface and acting along the x, y and z directions, respectively. Similarly, $\bar{p}_x$, $\bar{p}_y$ and $\bar{p}_z$ are the end tractions per unit area of the undeformed cross-section specified at $x = 0$ and L, where L is the undeformed length of the beam. Besides $\bar{f}_x$, $\bar{f}_y$ and $\bar{f}_z$ are the body forces per unit of volume. Finally, denoting $\bar{u}_x$, $\bar{u}_y$ and $\bar{u}_z$ as displacements at the middle line.

5. Constitutive equations

The constitutive equations of symmetrically balanced laminates may be expressed in the terms of shell stress resultants in the following form [17]:

$$\begin{Bmatrix} N_{xx} \\ N_{xs} \\ N_{xn} \\ M_{xx} \\ M_{xs} \end{Bmatrix} = \begin{bmatrix} \bar{A}_{11} & 0 & 0 & 0 & 0 \\ 0 & \bar{A}_{66} & 0 & 0 & 0 \\ 0 & 0 & \bar{A}_{55}^{(H)} & 0 & 0 \\ 0 & 0 & 0 & \bar{D}_{11} & 0 \\ 0 & 0 & 0 & 0 & \bar{D}_{66} \end{bmatrix} \begin{Bmatrix} \varepsilon_{xx}^{(0)} \\ \gamma_{xs}^{(0)} \\ \gamma_{xn}^{(0)} \\ \kappa_{xx}^{(1)} \\ \kappa_{xs}^{(1)} \end{Bmatrix} \tag{23}$$

with

$$\bar{A}_{11} = A_{11} - \frac{A_{12}^2}{A_{22}}, \quad \bar{A}_{66} = A_{66} - \frac{A_{26}^2}{A_{22}}, \quad \bar{A}_{55}^{(H)} = A_{55}^{(H)} - \frac{\left(A_{45}^{(H)}\right)^2}{A_{44}^{(H)}},$$
$$\bar{D}_{11} = D_{11} - \frac{D_{12}^2}{D_{22}}, \quad \bar{D}_{66} = D_{66} - \frac{D_{26}^2}{D_{22}}, \tag{24}$$

where A_{ij}, D_{ij} and $A_{ij}^{(H)}$ are plate stiffness coefficients defined according to the lamination theory presented by Barbero [17]. The coefficient $\bar{D}_{16}$ has been neglected because of its low value for the considered laminate stacking sequence [20].

6. Principle of virtual work for thin-walled beams

Substituting Eqs. (16)–(20) into Eq. (21) and integrating with respect to s, one obtains the one-dimensional (1-D) expression for the virtual work equation given by

$$L_M + L_K + L_P = 0, \tag{25}$$

where L_M, L_k and L_p represent the virtual work contributions due to the inertial, internal and external forces, respectively. Their expressions are given below:

$$L_M = \int_0^L \rho \left[A \frac{\partial^2 u_0}{\partial t^2} \delta u_0 + I_z \frac{\partial^2 \theta_z}{\partial t^2} \delta \theta_z + I_y \frac{\partial^2 \theta_y}{\partial t^2} \delta \theta_y + C_w \frac{\partial^2 \theta}{\partial t^2} \delta \theta + A \frac{\partial^2}{\partial t^2} (v - z_0 \phi) \delta v \right.$$
$$\left. + A \frac{\partial^2}{\partial t^2} (w + y_0 \phi) \delta w + \frac{\partial^2}{\partial t^2} (-A z_0 v + A y_0 w + I_s \phi) \delta \phi \right] \mathrm{d}x, \tag{26}$$

where A is the cross-sectional area, I_z and I_y the principal moments of inertia of the cross-section, C_w the warping constant, I_s the polar moment with respect to the SR and ρ the mean density of the laminate:

$$L_K = \int_0^L \left\{ \delta u_0' N + \delta v' \left(Q_y + v' N \right) + \delta w' \left(Q_z + w' N \right) \right.$$
$$+ \delta \theta_z \left[-Q_y + \frac{1}{2} \left(Q_z y_0 - Q_y z_0 \right) \theta_y' - \frac{1}{2} T_{sv} \theta_y' - \frac{1}{2} B \theta_y'' \right] - \delta \theta_y'' \frac{1}{2} B \theta_z$$
$$+ \delta \theta_z' \left[-M_z + \left(M_y + N z_0 \right) \phi + \frac{1}{2} \left(Q_y z_0 - Q_z y_0 \right) \theta_y + \frac{1}{2} T_{sv} \theta_y \right]$$
$$+ \delta \theta_y \left[-Q_{z_0} + \frac{1}{2} \left(Q_y z_0 - Q_z y_0 \right) \theta_z' + \frac{1}{2} T_{sv} \theta_z' + \frac{1}{2} B \theta_z'' \right] + \delta \theta_z'' \frac{1}{2} B \theta_y$$

$$+\delta\theta_y'\left[-M_y-\left(M_z+Ny_0\right)\phi+\frac{1}{2}\left(Q_z y_0-Q_y z_0\right)\theta_z-\frac{1}{2}T_{sv}\theta_z\right]$$
$$+\delta\phi\left[\left(M_y+Nz_0\right)\theta_z'-\left(M_z+Ny_0\right)\theta_y'\right]+\delta\phi'\left(T_w+T_{sv}+B_1\phi'\right)+\delta\theta' B-\delta\theta T_w\Big\}\,\mathrm{d}x, \quad (27)$$

$$L_P=\int_0^L\left(-q_x\delta u_0-q_y\delta v-q_z\delta w+m_z\delta\theta_z+m_y\delta\theta_y-b\delta\theta-m_x\delta\phi\right)\mathrm{d}x$$
$$+\left|-\bar{N}\delta u_0-\bar{B}\delta\theta-\bar{Q}_y\delta v-\bar{Q}_z\delta w+\delta\theta_z\left[\bar{M}_z-\left(\bar{M}_y+\bar{N}z_0\right)\phi\right]\right.$$
$$+\delta\theta_y\left[\bar{M}_y+\left(\bar{M}_z+\bar{N}y_0\right)\phi\right]+\delta\phi\left[-\bar{M}_x-\left(\bar{M}_y+\bar{N}z_0\right)\theta_z+\left(\bar{M}_z+\bar{N}y_0\right)\theta_y\right]\Big|_{x=0}^{x=L}. \quad (28)$$

7. Beam forces

In the above expressions, the following 1-D beam forces, in terms of the shell forces, have been defined:

$$N=\int N_{xx}\,\mathrm{d}s,\quad M_Y=\int\left(N_{xx}\bar{Z}+M_{xx}\frac{\mathrm{d}Y}{\mathrm{d}s}\right)\mathrm{d}s,\quad M_Z=\int\left(N_{xx}\bar{Y}-M_{xx}\frac{\mathrm{d}Z}{\mathrm{d}s}\right)\mathrm{d}s,$$
$$Q_Z=\int\left(N_{xs}\frac{\mathrm{d}Z}{\mathrm{d}s}+N_{xn}\frac{\mathrm{d}Y}{\mathrm{d}s}\right)\mathrm{d}s,\quad Q_Y=\int\left(N_{xs}\frac{\mathrm{d}Y}{\mathrm{d}s}-N_{xn}\frac{\mathrm{d}Z}{\mathrm{d}s}\right)\mathrm{d}s,$$
$$T_w=\int(N_{xs}(r-\psi)+N_{xn}l)\,\mathrm{d}s,\quad B=\int\left(N_{xx}\omega_p-M_{xx}l\right)\mathrm{d}s,$$
$$T_{\mathrm{sv}}=\int(N_{xs}\psi-2M_{xs})\,\mathrm{d}s,\quad B_1=\int\left[N_{xx}\left(Y^2+Z^2\right)-2M_{xx}r\right]\mathrm{d}s, \quad (29)$$

where the integration is carried out over the entire length of the mid-line contour. N corresponds to the axial force, Q_y and Q_z to shear forces, M_y and M_z to bending moments about y- and z-axis, respectively, B to the bimoment, T_w to the flexural–torsional moment, T_{sv} to the Saint-Venant torsional moment and B_1 to a high-order stress resultant, which contributes to the torque.

The relationships among the generalized beam forces and the generalized strains characterizing the behavior of the beam are obtained by substituting Eqs. (16)–(20) into Eq. (23), and the results into Eq. (29). This constitutive law can be expressed in terms of a beam stiffness matrix [D] as defined in Appendix A.

8. Equations of motion

Taking variations with respect to the generalized displacement u_0, θ_z, v, θ_y, w, θ, ϕ as indicated in Eqs. (26), (27) and (28), one obtains the equations of motion. In the case of a beam subjected to an axial excitation, the equations of motion can be reduced considering only the interaction of the longitudinal motion on the other motions. Therefore, in this case we obtain

$$-N'+\rho A\frac{\partial^2 u_0}{\partial t^2}=0, \quad (30a)$$

$$M_z'-Q_y\,\underline{-Nz_0\phi'}+\rho I_z\frac{\partial^2\theta_z}{\partial t^2}=0, \quad (30b)$$

$$-Q_y'-Nv''+\rho A\left(\frac{\partial^2 v}{\partial t^2}-z_0\frac{\partial^2\phi}{\partial t^2}\right)=0, \quad (30c)$$

$$M_y'-Q_z\,\underline{+Ny_0\phi'}+\rho I_y\frac{\partial^2\theta_y}{\partial t^2}=0, \quad (30d)$$

$$-Q_z' - Nw'' + \rho A\left(\frac{\partial^2 w}{\partial t^2} + y_0 \frac{\partial^2 \phi}{\partial t^2}\right) = 0, \tag{30e}$$

$$-B' - T_w + \rho C_w \frac{\partial^2 \theta}{\partial t^2} = 0, \tag{30f}$$

$$-T_w' - T_{sv}' + N\underline{\left(z_0\theta_z' - y_0\theta_y' - \frac{I_s}{A}\phi''\right)} + \rho A\left(y_0\frac{\partial^2 w}{\partial t^2} - z_0\frac{\partial^2 v}{\partial t^2} + \frac{I_s}{A}\frac{\partial^2 \phi}{\partial t^2}\right) = 0 \tag{30g}$$

subjected to the following boundary conditions (at $x = 0, L$)

$$N - \bar{N} = 0 \quad \text{or} \quad \delta u_0 = 0, \tag{31a}$$

$$-M_z + Nz_0\phi \underline{-\bar{N}z_0\phi} = 0 \quad \text{or} \quad \delta\theta_z = 0, \tag{31b}$$

$$Q_y + v'N = 0 \quad \text{or} \quad \delta v = 0, \tag{31c}$$

$$-M_y \underline{-Ny_0\phi} + \bar{N}y_0\phi = 0 \quad \text{or} \quad \delta\theta_y = 0, \tag{31d}$$

$$Q_z + w'N = 0 \quad \text{or} \quad \delta w = 0, \tag{31e}$$

$$B = 0 \quad \text{or} \quad \delta\theta = 0, \tag{31f}$$

$$T_w + T_{sv} - \bar{N}\underline{\left(z_0\theta_z - y_0\theta_y - \frac{I_s}{A}\phi'\right)} = 0 \quad \text{or} \quad \delta\phi = 0. \tag{31g}$$

In some previous papers, the displacement field equation (4) is simplified significantly, by introducing the first-order approximations [20]. However, considering this approximation, the components of the generalized displacements are linear functions of the displacements u_0, v, w, θ_z, θ_z, ϕ and θ, so that some important terms in the nonlinear strains equations (16)–(20) may be lost. These may lead to incorrect expressions for the movements equations (30) and inaccurate predictions of the dynamic behavior of thin-walled beams. The terms underlined in Eqs. (30b), (30d) and (30g) are those that disappear in a first-order formulation [20], and appear in a different way in Eqs. (30c), (30e) and (30g).

9. Dynamic stability

In this section, the dynamic stability of a simply supported thin-walled composite beam is analyzed considering an axial excitation in the form

$$P(t) = P_s + P_d \cos \varpi t, \tag{32}$$

where ϖ is the excitation frequency, $P_s = \alpha P_{cr}$, $P_d = \beta P_{cr}$, α is the static load factor, β is the dynamic load factor and P_{cr} is the critical load of the beam.

When the beam is excited in the axial (longitudinal) direction, and the interaction of this movement on the other motions is to be studied, the coupling of these various motions will depend on the symmetry of the cross-section analyzed.

The differential expression equation (30a) corresponding to the longitudinal movement is generally solved disregarding the longitudinal inertia forces, in the following form:

$$N = -P(t). \tag{33}$$

This procedure is followed in this section. However, in some cases the longitudinal inertia forces can substantially influence the dynamic stability of a beam. This effect is explained in Section 10.

The differential equations (30b)–(30g) are discretized by means of the following functions:

$$v = v_0(t)\,\sin\left(\frac{k\pi x}{L}\right),\quad \theta_z = \theta_{z_0}(t)\cos\left(\frac{k\pi x}{L}\right),$$
$$w = w_0(t)\,\sin\left(\frac{k\pi x}{L}\right),\quad \theta_y = \theta_{y_0}(t)\cos\left(\frac{k\pi x}{L}\right),$$
$$\phi = \phi_0(t)\,\sin\left(\frac{k\pi x}{L}\right),\quad \theta = \theta_0(t)\cos\left(\frac{k\pi x}{L}\right)\quad (k = 1, 2, 3, \ldots), \tag{34}$$

where $v_0(t)$, $\theta_{z0}(t)$, $w_0(t)$, $\theta_{y0}(t)$, $\phi_0(t)$ and $\theta_0(t)$ are the associated displacement amplitudes which are time dependent.

The formal substitution of Eqs. (33) and (34) into Eqs. (30b)–(30g) leads to a system of ordinary differential equations, which can be expressed in a compact form by using matrix notations as

$$\mathbf{M}\,\ddot{U} + [\mathbf{K} - P(t)\mathbf{S}]U = 0, \tag{35}$$

where $\{U\}^t = \left\{\theta_{z_0}(t); v_0(t); \theta_{y_0}(t); w_0(t); \theta_0(t); \phi_0(t)\right\}$,

$$\mathbf{M} = \begin{bmatrix} \rho I_z & 0 & 0 & 0 & 0 & 0 \\ & \rho A & 0 & 0 & 0 & -z_0\rho A \\ & & \rho I_y & 0 & 0 & 0 \\ & & & \rho A & 0 & y_0\rho A \\ & \text{SYM} & & & \rho C_w & 0 \\ & & & & & \rho A \end{bmatrix},\quad \mathbf{S} = \begin{bmatrix} 0 & 0 & 0 & 0 & 0 & -z_0\lambda_k \\ & \lambda_k^2 & 0 & 0 & 0 & 0 \\ & & 0 & 0 & 0 & y_0\lambda_k \\ & & & \lambda_k^2 & 0 & 0 \\ & \text{SYM} & & & 0 & 0 \\ & & & & & \frac{I_s}{A}\lambda_k^2 \end{bmatrix}, \tag{36a,b}$$

$$\mathbf{K} = \begin{bmatrix} \widehat{EI}_z\lambda_k^2 + \widehat{GS}_{yy} & -\widehat{GS}_{yy}\lambda_k & 0 & 0 & 0 & 0 \\ & \widehat{GS}_{yy}\lambda_k^2 & 0 & 0 & 0 & 0 \\ & & \widehat{EI}_y\lambda_k^2 + \widehat{GS}_{zz} & -\widehat{GS}_{zz}\lambda_k & \widehat{GS}_{wz} & -\widehat{GS}_{wz}\lambda_k \\ & & & \widehat{GS}_{zz}\lambda_k^2 & -\widehat{GS}_{wz}\lambda_k & \widehat{GS}_{wz}\lambda_k^2 \\ & \text{SYM} & & & \widehat{EC}_w\lambda_k^2 + \widehat{GS}_{ww} & -\widehat{GS}_{ww}\lambda_k \\ & & & & & \left(\widehat{GJ} + \widehat{GS}_{ww}\right)\lambda_k^2 \end{bmatrix}, \tag{36c}$$

where [**M**] denotes the mass matrix, [**K**] is the elastic stiffness matrix, [**S**] is the geometric matrix and $\lambda_k = k\pi x/L$.

Then, the problem concerning the determination of frequencies of free vibration of a beam loaded by a constant longitudinal force, it is expressed:

$$\left|\boldsymbol{K} - P_s\boldsymbol{S} - \Omega^2\boldsymbol{M}\right| = 0, \tag{37}$$

while the problem of the determination of frequencies of free vibration of an unloaded beam leads to the following equation:

$$\left|\boldsymbol{K} - \boldsymbol{M}\omega^2\right| = 0 \tag{38}$$

and the buckling problem can be analyzed from the following equation:

$$|\boldsymbol{K} - P_s\boldsymbol{S}| = 0. \tag{39}$$

9.1. Principal parametric resonance

The unstable boundaries for the thin-walled composite beam subjected to an axial periodic load are studied in this section. In the classification of parametric resonance, if ϖ is the excitation frequency and Ω_i the natural frequency of the ith mode, parametric resonance of "first kind" is said to occur when $\varpi/2\Omega \approx 1/r$, $r = 1,2,\ldots$ while parametric resonance of the "second kind" is said to occur when $\varpi/(\Omega_k + \Omega_j) \approx 1/r$, $r = 1,2,\ldots$ ($k \neq j$). In both cases the situation where $r = 1$ is generally the only one of practical importance. Usually, the parametric resonance of the first kind is termed "parametric resonance", whereas the second kind is referred as "combination resonance", because it involves two different frequencies. In this paper the study is only concentrated in the case of parametric resonance.

Finding the boundaries of the regions of instability reduces to the determination of the conditions under which the differential equation (35) of the system has periodic solutions with period $2\pi/\varpi$ and $4\pi/\varpi$ [3]. For the principal region, which is a half-subharmonic, one looks for a solution with a period which is twice the forcing frequency: i.e., $4\pi/\varpi$.

The condition for the existence of solutions can be expressed in the following infinite determinant form [3]:

$$\begin{vmatrix} \mathbf{K} - \mathbf{S}\left(P_s \pm \frac{1}{2}P_d\right) - \frac{1}{4}\varpi^2\mathbf{M} & -\frac{1}{2}P_d\mathbf{S} & 0 & \cdots \\ & \mathbf{K} - P_s\mathbf{S} - \frac{9}{4}\varpi^2\mathbf{M} & -\frac{1}{2}P_d\mathbf{S} & \cdots \\ \text{SYM} & & \mathbf{K} - P_s\mathbf{S} - \frac{25}{4}\varpi^2\mathbf{M} & \cdots \\ \cdots\cdots & \cdots\cdots & \cdots\cdots & \cdots \end{vmatrix} = 0. \tag{40}$$

The boundaries of the instability regions lying near $\varpi = 2\Omega$ can be determined with sufficient accuracy considering the first leading diagonal term:

$$\left|\mathbf{K} - \mathbf{S}\left(P_s \pm \tfrac{1}{2}P_d\right) - \tfrac{1}{4}\varpi^2\mathbf{M}\right| = 0. \tag{41}$$

10. Influence of forced and parametrically excited vibrations

In the previously developed theory, the longitudinal force in the beam is equal to the external force acting in the end of the beam and therefore the longitudinal vibrations are neglected. Such an assumption is valid to a certain extent when the exciting frequency is small in comparison with the frequency ω_L of the free longitudinal vibrations. However, for beams with small slenderness ratio or particular lamination sequence, the frequency at which a parametric resonance occurs, can be the same order as the natural frequency of the longitudinal vibrations. To consider this effect is necessary to substitute the constitutive expression corresponding to the axial force N into Eq. (30a) and solving for the displacement u_0:

$$-\widehat{EA}\frac{\partial^2 u_0}{\partial x^2} + \rho A\frac{\partial^2 u_0}{\partial t^2} = 0. \tag{42}$$

The solution of this equation is easily obtained by considering the boundary condition equation (31a)

$$u_0(x,t) = \frac{P_s x}{\widehat{EA}} + \frac{P_d \sin vx}{v\widehat{EA}\cos vL}\cos \varpi t, \tag{43}$$

where

$$v = \varpi\sqrt{\frac{\rho A}{\widehat{EA}}}. \tag{44}$$

Substituting Eq. (43) into Eqs. (30b)–(30g) and applying the same methodology previously explained, Eq. (41) can be expressed in the following form:

$$\left|\mathbf{K} - \mathbf{S}\left(P_s \pm \frac{1}{2}P_d\frac{\tan vL}{vL}\right) - \frac{1}{4}\varpi^2\mathbf{M}\right| = 0. \tag{45}$$

Solving Eq. (45) the main regions of instability considering the influence of the longitudinal vibration are obtained.

11. Applications and numerical results

The purpose of this section is to apply the present theoretical model in order to study the dynamic stability of simply supported thin-walled composite beams. The influence of longitudinal vibrations and the effect of shear deformation on the regions of instability are analyzed. In the following numerical results, the shear effect on the thickness $\gamma_{xn}^{(0)}$ has been neglected because its consideration conduces to inaccurate results for thin-walled sections, as explained by Piovan and Cortínez [27]. They showed that the inclusion of the in-thickness shear deformation effect increases erroneously the rigidity instead of flexibilizing the beam behavior. Different cross-sectional shapes, laminate schemes and beam lengths are considered to perform the numerical analysis. The analyzed material is graphite-epoxy (AS4/3501) whose properties are $E_1 = 144\,\text{GPa}$, $E_2 = 9.65\,\text{GPa}$, $G_{12} = 4.14\,\text{GPa}$, $G_{13} = 4.14\,\text{GPa}$, $G_{23} = 3.45\,\text{GPa}$, $\nu_{12} = 0.3$, $\nu_{13} = 0.3$, $\nu_{23} = 0.5$, $\rho = 1389\,\text{kg/m}^3$. The analyzed cross-sections are shown in Fig. 2.

In all the results presented below, the value of the static load parameter is adopted $\alpha = 0.5$, and the excitation frequency ϖ is scaled with the lowest frequency value of parametric resonance (that is the double of the frequency value of the vibration mode first $2\Omega_1$).

11.1. Bisymmetric open section

The example considered is a simply supported bisymmetric-I section whose geometric properties are $L = 6\,\text{m}$, $h = 0.6\,\text{m}$, $b = 0.6\,\text{m}$, $e = 0.03\,\text{m}$. In this example ($y_0 = z_0 = 0$), the system equations are uncoupled. Therefore, there are three main modes of vibration corresponding either to bending or to torsion. In this case, the lowest frequency corresponds to the lateral flexural mode (y-direction), while the highest frequency of vibration corresponds to the vertical flexural mode (z-direction).

Instability regions are shown in the Figs. 3–5, for different laminate stacking sequences. The critical load of the beam corresponding to the flexural mode can be easily obtained by means of Eq. (38) (as explained by the authors in Ref. [15]):

$$P_{cr} = \frac{\pi^2}{L^2}\frac{\widehat{EI}_z\widehat{GS}_y}{\widehat{GS}_y + \widehat{EI}_z\pi^2/L^2}, \tag{46}$$

where $\widehat{EI}_z$ is the flexural stiffness, $\widehat{GS}_z$ and $\widehat{GS}_y$ are shear stiffnesses of a composite beam. The definitions of these stiffnesses are given in Appendix A.

It is observed that the widest unstable region corresponds to the first mode (or to the first frequency of parametric resonance), while the smallest region belongs to the third mode (or third frequency of parametric resonance). The size of the principal unstable region (first mode) keeps practically constant for the different sequences of lamination analyzed. While the second parametric region (2° mode) decreases considerably for a lamination sequence {*45/-45/-45/45*}. The second parametric resonance frequency, for the same lamination, is

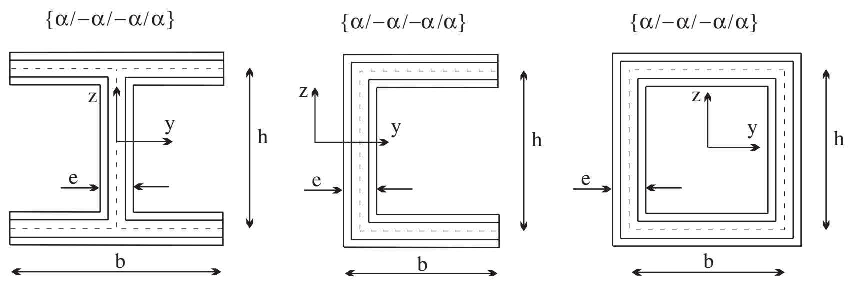

Fig. 2. Analyzed cross-sectional shapes.

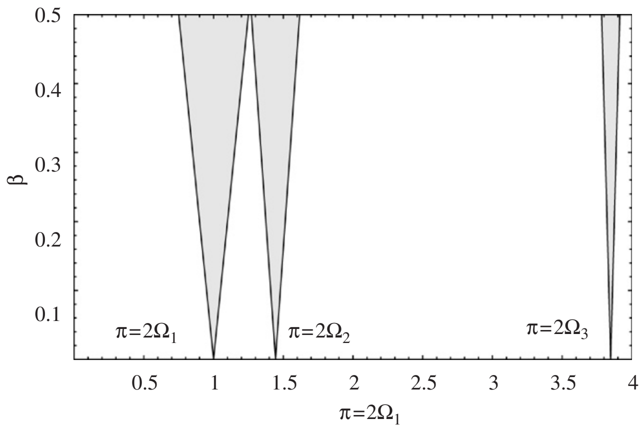

Fig. 3. Regions of dynamic instability for a bisymmetric beam {*0/0/0/0*}.

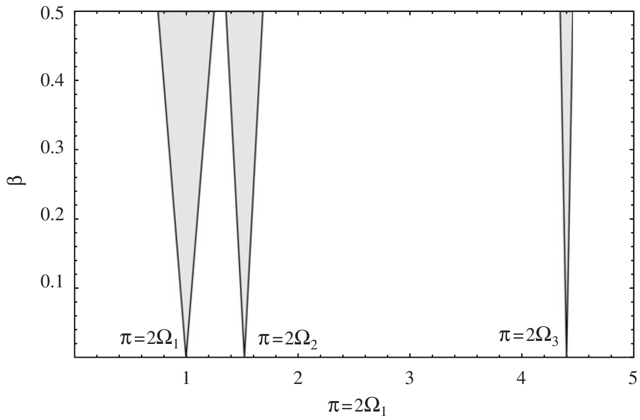

Fig. 4. Regions of dynamic instability for a bisymmetric beam {*0/90/90/0*}.

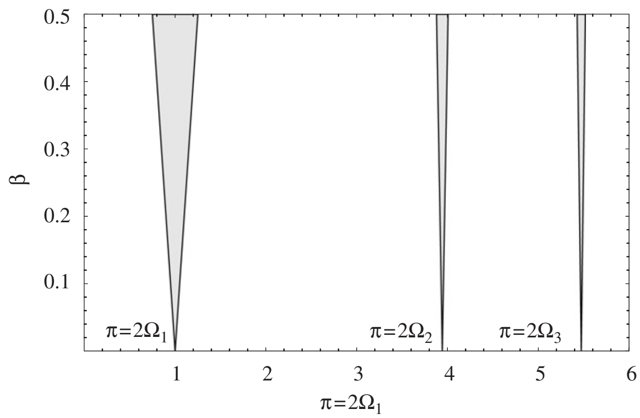

Fig. 5. Regions of dynamic instability for a bisymmetric beam {*45/-45/-45/45*}.

more distant from the principal region. This phenomenon is due to the torsional stiffness is larger in comparison with the other laminations.

In Table 1, natural frequencies are given considering two models: the present theory (model I) and results obtained by neglecting shear flexibility (model II). The shear deformation effect reduces considerably the

Table 1
Natural frequencies for a bisymmetric beam (Hz), $\alpha = 0.5$

Frequencies	{0/0/0/0}		{0/90/90/0}		{45/-45/-45/45}	
	Model I	Model II	Model I	Model II	Model I	Model II
Ω_1	18.66	19.96	13.88	14.41	6.24	6.24
Ω_2	26.96	28.23	21.11	21.59	24.55	24.55
Ω_3	71.81	106.37	60.99	77.84	34.08	34.31
ω_L	424.24		310.60		136.97	

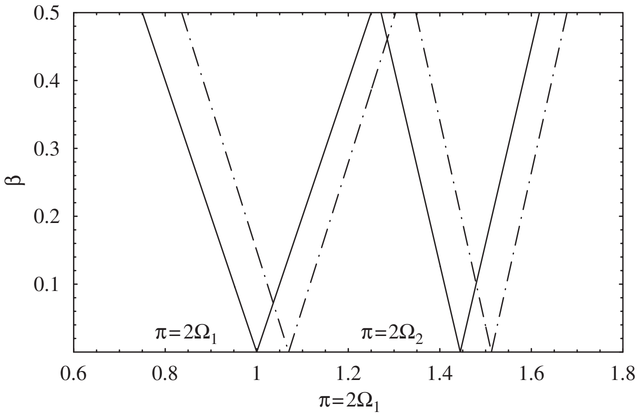

Fig. 6. First and second instable regions, lamination {*0/0/0/0*}, (—) present theory, (–·–) neglecting shear flexibility.

vibration frequency values when the lamination {*0/0/0/0*} is used, while this effect has no influence for the lamination {*45/-45/-45/45*}.

It is important to mention that the influence of the longitudinal inertia is negligible in all the laminations analyzed, due to the exciting frequency is far from the longitudinal natural frequencies of the beam (ω_L).

On the hand, the influence of shear deformation on the dynamic behavior of composite beams is analyzed for the lamination sequence {*0/0/0/0*}. The unstable regions of the first and second parametric resonance are shown in Fig. 6, where two models are compared: the present theory (considering shear flexibility) and results obtained by neglecting shear flexibility. The width of the regions does not change for both models. However, when shear deformation is neglected the unstable region moves toward the right, originated by an increase in the parametric frequency values.

11.2. Monosymmetric open cross-section

The considered example is a monosymmetric channel section, the geometric properties are $L = 6$ m, $h = 0.6$ m, $b = 0.6$ m, $e = 0.03$ m. In this case ($z_0 = 0$), the system of equations corresponding to y-direction (v transversal displacement) are therefore uncoupled. Thus, when the beam is subjected to a longitudinal force, it is possible to excite the beam parametrically in either to bending modes in y-direction (v) or in flexural–torsional mode of vibration (w and ϕ. For the cross-section analyzed, the flexural–torsional mode presents the smallest parametric frequency value. Therefore, the excitation frequency is scaled with the value of this last frequency.

Regions of dynamic instability for the composite channel-beam are shown in Figs. 7 and 8, considering the lamination sequences {*0/0/0/0*}, {*0/90/90/0*} and {*45/-45/-45/45*}, respectively. The first and third instability regions (Ω_1 and Ω_3) correspond to the flexural–torsional mode, while the second region corresponds to the

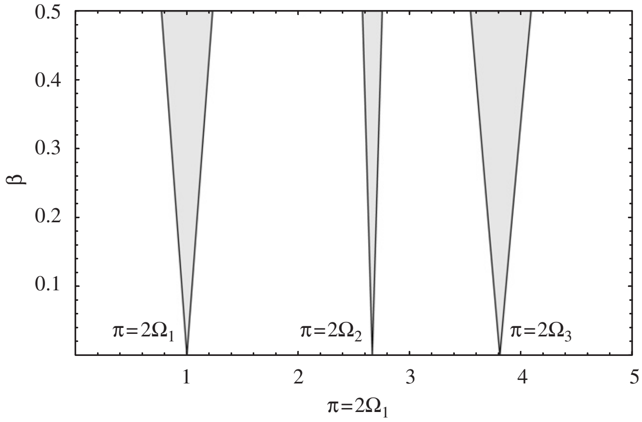

Fig. 7. Regions of dynamic instability for a channel-beam {*0/0/0/0*}.

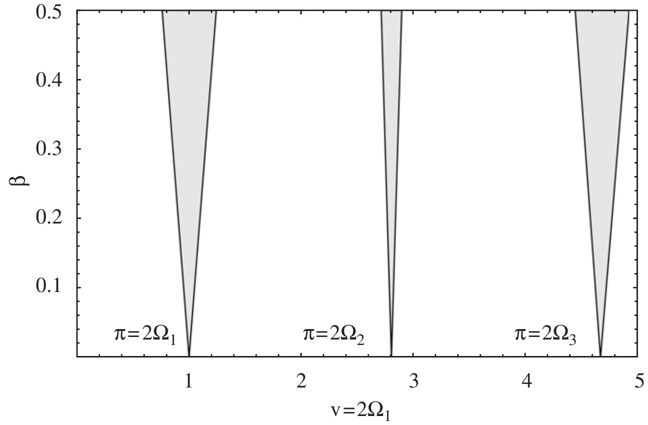

Fig. 8. Regions of dynamic instability for a channel-beam {*0/90/90/0*}.

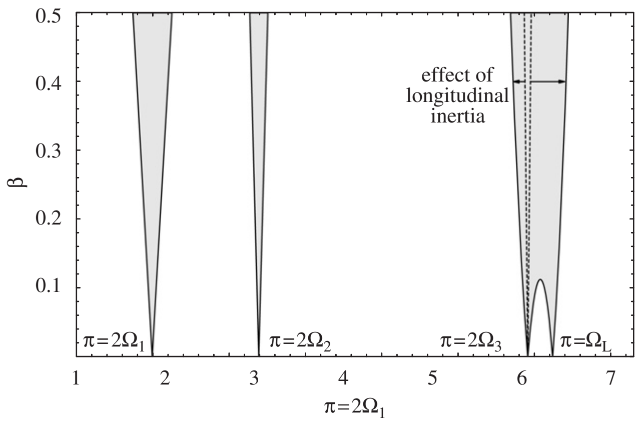

Fig. 9. Regions of dynamic instability for a channel-beam {*45/-45/-45/45*}, (—) present theory, (- - -) neglecting longitudinal inertia.

uncoupled flexural mode (Ω_2). The critical load of the beam corresponding to the flexural–torsional mode can be obtained by means of Eq. (38) [15].

From the figures, one can observe that the sizes of the unstable region of the first and second modes are similar for the different laminations. However, the third region, corresponding to the second flexural–torsional mode, is wider for the lamination {*45/-45/-45/45*} than those obtained for the other laminations (see Fig. 9). This phenomenon is due to that the exciting frequency is near to the longitudinal natural frequencies of the beam (ω_L). The influence of the longitudinal inertia enlarges the third region, which certainly is composed by two regions, one of them lies near $\varpi = 2\Omega_3$ ($\Omega_3/\Omega_1 = 5.92$); and the second lies near $\varpi = \omega_L$ ($\omega_L/2\Omega_1 = 6.24$). Fig. 9 shows comparative results between the unstable regions obtained by disregarding (which is much narrower than the resultant region) and considering the influence of the longitudinal vibration.

In Table 2, natural frequencies are given for the different laminations, considering the effect of shear deformation. One can observe from this table, a noticeable difference between both models when the lamination sequence {*0/0/0/0*} is used. This discrepancy can reach a percentage of about 110% for the frequency value Ω_3.

11.3. Bisymmetric closed section

In this example, a bisymmetric box-beam is used to study the dynamic behavior, whose geometric properties are $L = 6\,\text{m}$, $h = 0.6\,\text{m}$, $b = 0.6\,\text{m}$, $e = 0.03\,\text{m}$. In the similar way as the example (10.1), $y_0 = z_0 = 0$, there are three vibration modes corresponding either to bending or to torsion. However in this case, the flexural stiffnesses are the same order, for that reason bending frequencies are also the same. The lower frequency corresponds to the lateral and vertical flexural mode, while the higher frequency of vibration corresponds to the torsional mode.

In this example, the influence of the static load parameter α is analyzed. Regions of dynamic instability for the composite box-beam are shown in Figs. 10–12, considering three different values of the parameter $\alpha = 0.5$,

Table 2
Natural frequencies for a channel-beam (Hz), $\alpha = 0.5$

Frequencies	{*0/0/0/0*}		{*0/90/90/0*}		{*45/-45/-45/45*}	
	Model I	Model II	Model I	Model II	Model I	Model II
Ω_1	25.08	30.89	19.16	21.70	10.97	10.99
Ω_2	66.77	85.29	53.67	62.06	26.27	26.37
Ω_3	95.46	200.81	89.33	146.92	64.91	65.95
ω_L	424.24		310.60		136.97	

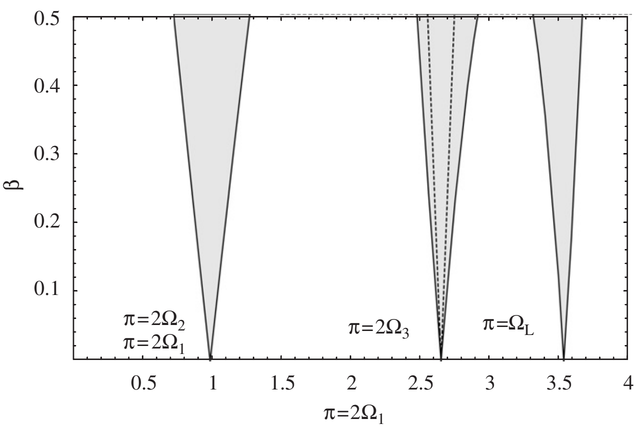

Fig. 10. Regions of dynamic instability for a box-beam $\alpha = 0.5$, (—) present theory, (- - -) neglecting longitudinal inertia.

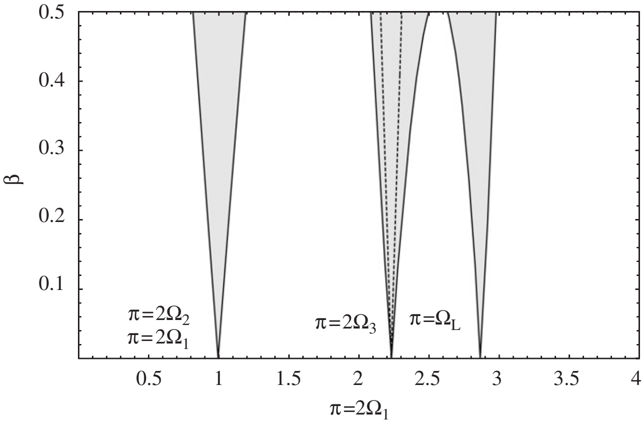

Fig. 11. Regions of dynamic instability for a box-beam $\alpha = 0.25$, (—) present theory, (- - -) neglecting longitudinal inertia.

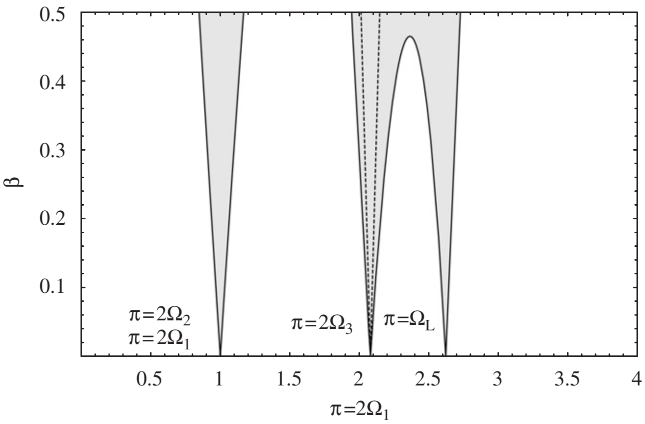

Fig. 12. Regions of dynamic instability for a box-beam $\alpha = 0.10$, (—) present theory, (- - -) neglecting longitudinal inertia.

Table 3
Natural frequencies for a box-beam (Hz) {*0/90/90/0*}

Frequencies	$\alpha = 0.1$	$\alpha = 0.25$	$\alpha = 0.5$
Ω_1, Ω_2	59.33	54.16	44.22
Ω_3	123.21	120.79	116.65
ω_L		310.59	

$\alpha = 0.25$ and $\alpha = 0.1$, respectively, for a lamination sequence {*0/90/90/0*}. The first region represents the flexural mode either vertical or lateral and the second region represents the torsional mode. The third region that appears in the figures represents the influence of the longitudinal vibration, which in this case is near to the unstable boundaries corresponding to torsional mode. It is observed from the figures that the first unstable region for $\alpha = 0.1$ (Fig. 12) is narrower than those corresponding to the higher static load parameter. However, the width of the second region ($\varpi = 2\Omega_3$) enlarges when the static load parameter increases, due to the influence of the longitudinal inertia. Consequently, the region of dynamic instability is composed by two regions, in the same way as the previous example for the lamination {*45/-45/-45/45*} (Fig. 9).

In Table 3, natural frequencies are given for the different load parameter values, considering shear deformation and a lamination sequence {*0/90/90/0*}. As the load parameter α increases, the frequencies values decrease. For that reason, the effect of longitudinal vibration has more influence on dynamic behavior for the smallest value of the parameter α.

The unstable regions that are obtained disregarding the longitudinal inertia are smaller than those obtained with the present theory. Therefore, its discard results, inadvertently, in a less critical behavior than in the case of its incorporation.

12. Conclusions

The equations of motion of axially oscillating beam are derived by means of a geometrically nonlinear second-order theory. The formulation is based on the context of a rational small strain and moderate rotation theory of thin-walled composite beams, through the adoption of a shear deformable displacement field (accounting for bending and warping shear). The given beam model is 1-D and is valid for bi-symmetric and mono-symmetric cross-sections either open or closed.

The dynamic stability of a simply supported thin-walled composite beam subjected to an axial periodic force has been studied. The dynamic stability analysis of the system is performed by employing the Hill's method of infinite determinants, which has been extensively investigated by Bolotin [3].

From the numerical results obtained, it is found that the regions of instability dynamic are generally wider for the first frequency of parametric resonance, and they decrease in their size as the resonance frequency value increases. However, the size of the unstable regions can vary depending on the influence of the longitudinal inertia. The influence of the interaction between the forced vibration and the parametrically excited vibrations on the unstable regions is considerable when the excitation frequency is the same order than the frequency value of the free longitudinal vibration. Moreover, this effect depends on the stacking sequence and on the parameter of static load. For example, this effect is noticeable in the case of a channel-beam with lamination {*45/-45/-45/45*} and insignificant for the other laminations.

On the other hand, the shear deformation effect has been investigated. The discard of transverse shear results in an overprediction of the resonance behavior, in the sense of the shift of the domain of instability toward larger excitation frequencies. This effect is more important when one of the material axes coincides with the beam axis.

Acknowledgments

The present study was sponsored by Secretaría de Ciencia y Tecnología, Universidad Tecnológica Nacional, and by CONICET. The present paper is part of the doctoral thesis presented by Sebastián Machado at Departamento de Ingeniería corresponding to the Universidad Nacional del Sur.

Appendix A. Constitutive law

The constitutive law for a bisymmetric beam is defined in the following form:

$$\{f_g\} = [D]\{\Delta\}, \tag{A.1}$$

$$\{f_g\} = \begin{bmatrix} N & M_y & M_z & B & Q_y & Q_z & T_w & T_{sv} & B_1 \end{bmatrix}^{\mathrm{T}}, \tag{A.2}$$

$$\{\Delta\} = \begin{bmatrix} \varepsilon_{D1} & \varepsilon_{D2} & \varepsilon_{D3} & \varepsilon_{D4} & \varepsilon_{D5} & \varepsilon_{D6} & \varepsilon_{D7} & \varepsilon_{D8} & \varepsilon_{D9} \end{bmatrix}^{\mathrm{T}}. \tag{A.3}$$

Where $\{f_g\}$ is the vector of generalized forces, $\{\Delta\}$ is the vector of the generalized strains and $[D]$ is a symmetric matrix (9×9):

$$\varepsilon_{D1} = u'_o + \tfrac{1}{2}\left(v'^2 + w'^2\right) - y_0\theta'_y\phi + z_0\theta'_z\phi,$$
$$\varepsilon_{D2} = -\theta'_z - \theta'_y\phi,$$

$$\begin{aligned}
\varepsilon_{D3} &= -\theta_y' + \theta_z'\phi, \\
\varepsilon_{D4} &= \theta' - \tfrac{1}{2}\left(\theta_z\theta_y'' - \theta_y\theta_z''\right), \\
\varepsilon_{D5} &= v' - \theta_z - z_0\tfrac{1}{2}\left(\theta_z\theta_y' - \theta_y\theta_z'\right), \\
\varepsilon_{D6} &= w' - \theta_y + y_0\tfrac{1}{2}\left(\theta_z\theta_y' - \theta_y\theta_z'\right), \\
\varepsilon_{D7} &= \phi' - \theta, \\
\varepsilon_{D8} &= \phi' - \tfrac{1}{2}\left(\theta_z\theta_y' - \theta_y\theta_z'\right), \\
\varepsilon_{D9} &= \tfrac{1}{2}\phi'^2,
\end{aligned} \tag{A.4}$$

$$D = \begin{bmatrix}
\widehat{EA} & 0 & 0 & 0 & 0 & 0 & 0 & 0 & \widehat{EI}_0 \\
0 & \widehat{EI}_y & 0 & 0 & 0 & 0 & 0 & 0 & 0 \\
0 & 0 & \widehat{EI}_z & 0 & 0 & 0 & 0 & 0 & 0 \\
0 & 0 & 0 & \widehat{EC}_w & 0 & 0 & 0 & 0 & 0 \\
0 & 0 & 0 & 0 & \widehat{GS}_y & 0 & 0 & 0 & 0 \\
0 & 0 & 0 & 0 & 0 & \widehat{GS}_z & 0 & 0 & 0 \\
0 & 0 & 0 & 0 & 0 & 0 & \widehat{GS}_w & 0 & 0 \\
0 & 0 & 0 & 0 & 0 & 0 & 0 & \widehat{GJ} & 0 \\
\widehat{EI}_0 & 0 & 0 & 0 & 0 & 0 & 0 & 0 & \widehat{EI}_R
\end{bmatrix}. \tag{A.5}$$

The elements of the symmetric matrix $[D]$ are given by the following contour integrals:

$$\begin{aligned}
\widehat{EA} &= \int \bar{A}_{11}\,\mathrm{d}s, \\
\widehat{EI}_y &= \int \left(\bar{A}_{11}Z^2 + \bar{D}_{11}Y'^2\right)\mathrm{d}s, \\
\widehat{EI}_z &= \int \left(\bar{A}_{11}Y^2 + \bar{D}_{11}Z'^2\right)\mathrm{d}s, \\
\widehat{EI}_w &= \int \left(\bar{A}_{11}\omega_p^2 + \bar{D}_{11}l^2\right)\mathrm{d}s, \\
\widehat{GS}_y &= \int \left(\bar{A}_{55}Z'^2 + \bar{A}_{66}Y'^2\right)\mathrm{d}s, \\
\widehat{GS}_z &= \int \left(\bar{A}_{55}Y'^2 + \bar{A}_{66}Z'^2\right)\mathrm{d}s, \\
\widehat{GJ} &= \int \left(\bar{A}_{66}\psi^2 + 4\bar{D}_{66}\right)\mathrm{d}s, \\
\widehat{EI}_R &= \int \left[\bar{A}_{11}\left(Y^2 + Z^2\right)^2 + 4\bar{D}_{11}r^2\right]\mathrm{d}s, \\
\widehat{EI}_0 &= \int \bar{A}_{11}\left(Y^2 + Z^2\right)\mathrm{d}s,
\end{aligned} \tag{A.6}$$

where

$$Y' = \frac{\mathrm{d}Y}{\mathrm{d}s}, \quad Z' = \frac{\mathrm{d}Z}{\mathrm{d}s}. \tag{A.7}$$

References

[1] R.M. Evan-Iwanowski, On the parametric response of structures, *Applied Mechanics Reviews* 18 (1965) 699–702.

[2] A.H. Nayfeh, D.T. Mook, *Nonlinear Oscillations*, Wiley, New York, 1979.

[3] V.V. Bolotin, *The Dynamic Stability of Elastic Systems*, Holden-Day, San Francisco, 1964.

[4] I.I. Gol'denblat, *Contemporary Problems of Vibrations and Stability of Engineering Structures*, Stroiizdat, Moscow, 1947.

[5] W.K. Tso, Parametric torsional stability of a bar under axial excitation, *Journal of Applied Mechanics* 35 (1868) 13–19.

[6] E. Mettler, *Dynamic Buckling, Handbook of Engineering Mechanics*, McGraw-Hill, New York, 1962.

[7] A.A. Ghobarah, W.K. Tso, Parametric stability of thin-walled beams of open section, *Journal of Applied Mechanics* 39 (1972) 201–206.

[8] V.V. Bolotin, On the parametric excitation of transverse vibrations, *Collection of Papers: Transverse Vibrations and Critical Velocities* 2 (1953) 5–44.

[9] C.H. Popelar, Dynamic stability of the flexural vibrations of a thin-walled beam, *International Journal of Solids and Structures* 5 (1969) 549–557.

[10] C.H. Popelar, Dynamic stability of thin-walled column, *Journal of the Engineering, Mechanics Division, Proceedings of the American Society of Civil Engineers* 98 (1972) 657–677.

[11] S.A. Hasan, A.D.S. Barr, Non-linear and parametric vibration of thin-walled beams of equal angle-section, *Journal of Sound and Vibration* 31 (1974) 25–47.

[12] T.W. Kim, J.H. Kim, Parametric instability of a cross-ply laminated beam with viscoelastic properties under a periodic force, *Composite Structures* 51 (2001) 205–209.

[13] C.Y. Lin, L.W. Chen, Dynamic stability of rotating composite beams with a viscoelastic core, *Composite Structures* 58 (2002) 185–194.

[14] P. Hagedorn, L.P. Koval, On the parametric stability of a Timoshenko beam subjected to a periodic axial load, *Ingenieur Archiv* 40 (1971) 211–220.

[15] S.P. Machado, V.H. Cortínez, Lateral buckling of thin-walled composite bisymmetric beams with prebuckling and shear deformation, *Engineering Structures* 27 (2005) 1185–1196.

[16] S.P. Machado, V.H. Cortínez, Non-linear model for stability of thin-walled composite beams with shear deformation, *Thin-walled Structures* 43 (2005) 1615–1645.

[17] E.J. Barbero, *Introduction to Composite Material Design*, Taylor & Francis, London, 1999.

[18] J.N. Reddy, *Mechanics of Laminated Composite Plates and Shells: Theory and Analysis*, second ed., CRC Press, Boca Raton, FL, 2004.

[19] Y.L. Pi, M.A. Bradford, Effects of approximations in analysis of beams of open thin-walled cross-section—part I: flexural–torsional stability, *International Journal for Numerical Methods in Engineering* 51 (2001) 757–772.

[20] V.H. Cortínez, M.T. Piovan, Vibration and buckling of composite thin-walled beams with shear deformability, *Journal of Sound and Vibration* 258 (4) (2002) 701–723.

[21] K. Bhaskar, L. Librescu, A geometrically non-linear theory for laminated anisotropic thin-walled beams, *International Journal of Engineering Science* 33 (9) (1995) 1331–1344.

[22] J.H. Argyris, An excursion into large rotations, *Computer Methods in Applied Mechanics and Engineering* 32 (1982) 85–155.

[23] F. Fraternali, L. Feo, On a moderate rotation theory of thin-walled composite beams, *Composites Part B—Engineering* 31 (2000) 141–158.

[24] V.H. Cortínez, R.E. Rossi RE, Dynamics of shear deformable thin-walled open beams subjected to initial stresses, *Revista Internacional sobre Métodos Numéricos para Cálculo y Diseño en Ingeniería* 14 (3) (1998) 293–316.

[25] S. Krenk, O. Gunneskov, Statics of thin-walled pre-twisted beams, *International Journal of Numerical Methods in Engineering* 17 (1981) 1407–1426.

[26] K. Washizu, *Variational Methods in Elasticity and Plasticity*, Pergamon Press, Oxford, 1968.

[27] M.T. Piovan, V.H. Cortínez, Transverse shear deformability in the dynamics of thin-walled composite beams: consistency of different approaches, *Journal of Sound and Vibration* 285 (2005) 721–733.